LANGMUIR

Article

pubs.acs.org/Langmuir

Investigating the Role of Phosphorylation in the Binding of Silaffin Peptide R5 to Silica with Molecular Dynamics Simulations

K. G. Sprenger,[†,#] Arushi Prakash,[†,#] Gary Drobny,[‡] and Jim Pfaendtner*[,†]

[†]Department of Chemical Engineering, University of Washington, Seattle, Washington 98105, United States

[‡]Department of Chemistry, University of Washington, Seattle, Washington 98195, United States

Supporting Information

ABSTRACT: Biomimetic silica formation, a process that is largely driven by proteins, has garnered considerable interest in recent years due to its role in the development of new biotechnologies. However, much remains unknown of the molecular-scale mechanisms underlying the binding of proteins to biomineral surfaces such as silica, or even of the key residue-level interactions between such proteins and surfaces. In this study, we employ molecular dynamics (MD) simulations to study the binding of R5—a 19-residue segment of a native silaffin peptide used for in vitro silica formation—to a silica surface. The metadynamics enhanced sampling method is used to converge the binding behavior of R5 on silica at both neutral (pH 7.5) and acidic (pH 5) conditions. The results show fundamental differences in the mechanism of binding between the two cases, providing unique insight into the pH-dependent ability of R5 and native silaffin to precipitate silica. We also study the effect of phosphorylation of serine residues in R5 on both the binding free energy to silica and the interfacial conformation of the peptide. Results indicate that phosphorylation drastically decreases the binding free energy and changes the structure of silica-adsorbed R5 through the introduction of charge and steric repulsion. New mechanistic insights from this work could inform rational design of new biomaterials and biotechnologies.

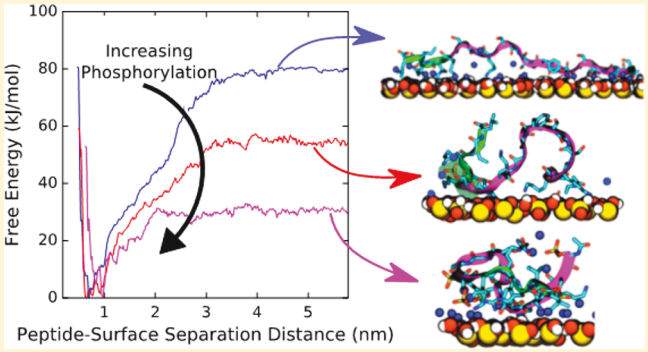

1. INTRODUCTION

Biosilicification is a complex process by which diatoms and sponges grow ornate silica exoskeletons. Biosilicification likely occurs through the self-assembly of proteins into a matrix, followed by the condensation of silicic acid to form silica nanostructures.[1] This process has been used to make silica nanostructures *in vitro* using not only silaffin proteins but long-chain polyamines, and specific silaffin domains.[1,2] In fact, the capacity of the 19-mer segment of silaffin named R5 (SSKKSGSYSGSKGSKRRIL) to precipitate silica and form nanostructures is well-documented.[1,3−6] It is highly desirable to obtain complete mechanistic control over this process for low-energy synthesis routes to produce nanomaterials of controlled morphology. To achieve this, it is important to determine the key interactions and driving forces governing biosilicification.

Several experimental studies have explored the conditions necessary for biosilicification to occur. Analysis of the silaffin sequence shows that post-translational modifications (PTMs)—namely the modification of lysine to long-chain polyamines, and serine and trimethyl-hydroxyl-lysine residues to phosphorylated residues—allow native silaffins to precipitate silica.[2,3,7−10] Indeed, phosphorylation was found necessary for any biosilicification activity to occur since the negatively charged phosphate groups countered the electrostatic repulsion between positively charged amine groups from neighboring R5 peptides, permitting them to self-assemble.[11] However, complete phosphorylation of serine residues can drastically decrease the tendency of these peptides to self-assemble.[11] Notably, the effect of phosphorylating the sequence of the peptides can be mimicked by the addition of negatively charged phosphate ions in the silicification environment, which likely promotes self-assembly by bridging the positively charged silaffin peptides together.[2,12,13] Other environmental variables, like pH, also affect biosilicification. Most strikingly, the pH for silica precipitation activity is different for synthetic R5 (pH 7) and native silaffin (pH 4−5). PTMs can also affect the pH sensitivity of R5.[14]

While these studies are primarily experimental, some computational investigations of the system have also been conducted. Some have investigated the large-scale assembly of peptides into matrices for silica condensation. For example, Lenoci et al. modeled silaffin peptides as coarse-grained beads that self-assembled via Brownian dynamics into a continuous

Special Issue: Early Career Authors in Fundamental Colloid and Interface Science

Received: August 13, 2017
Revised: October 5, 2017
Published: October 5, 2017

DOI: 10.1021/acs.langmuir.7b02868
Langmuir 2018, 34, 1199−1207

matrix with 15−25 nm cavities—at which size silica would likely assemble into nanostructures.[13] Eby et al. also used coarse-grained models of peptides, in addition to phosphate ions, and observed the formation of a scaffold-like structure consisting of a mixture of peptides and phosphate ions.[15] However, these studies were inconclusive about the atomic structure of the peptides in their models. Recently, Lutz et al. tried to decipher the molecular structure of R5 near silica aggregates at an air/water interface through fully atomistic molecular dynamics (MD) simulations.[16] They found that R5 loses its defined secondary structure upon interaction with extended silica sheets, and instead forms aggregates that interact with silica particles primarily through their C-terminal motifs (RRIL).[17] Despite these advances in obtaining a molecular level understanding of biosilicification through simulations, significant questions remain. Specifically, the atomic level interactions of R5/silaffin peptides with ions, and other peptides, are not well-characterized. Also, it is unclear how peptide−surface, peptide−peptide, and peptide−ion interactions individually affect the different stages of biosilicification.

Herein, we aim to provide new, high-resolution insights into the effect of PTMs of R5 and of pH on peptide/silica binding through MD simulations combined with the metadynamics enhanced sampling method. We simulated a single R5 peptide (and its mutants) on silica at pH 7.5 and pH 5. R5 mutants were designed with varying degrees of serine phosphorylation in the R5 sequence (at both neutral and acidic conditions) following the experimental study of Lechner et al.[11] In each case, the binding free energy to silica and the conformation of R5 at the interface were obtained. We simulated single-molecule systems, like other peptide−surface simulation studies,[18−20] to serve two purposes. First, exhaustive sampling of peptide aggregation at a solid/liquid surface is currently computationally prohibitive for the range of effects we consider in this work. Second, it highlights and ioslates the effect of environmental conditions on peptide−surface interactions without the added complexity of multi-peptide interactions. These results can be interpreted as the baseline for a bottom-up understanding of the biosilicification process that seeks to resolve the dominant driving forces that contribute to differences in silica precipitation and morphology under varying conditions, at the molecular scale.

2. METHODS

The structure of R5 (SSKKSGSYSGSKGSKRRIL) capped with a neutral acetyl group on the N-terminus was constructed with Visual Molecular Dynamics (VMD[21]) and modeled with the CHARMM36[22] force field. Two additional R5 sequences were constructed: "local phosphoserine (pS) R5" in which S14 was phosphorylated (SSKK-SGSYSGSKG*p*SKRRIL), and "global pS R5" in which every serine residue was replaced by a pS residue (*p*S*p*SKK*p*SG*p*SY*p*SG*p*SKG*p*S-KRRIL). At pH 7.5, the pS residues were parameterized to have a total charge of −2, such that overall charges were +6, + 4, and −8 for the unphosphorylated ("no pS"), local pS, and global pS R5 peptides, respectively. At pH 5 (pS charge −1), the peptides had overall charges of +6, + 5, and −1 for the no pS, local pS, and global pS R5 peptides, respectively. Charges from Steinbrecher et al.[23] were used for the pS residues at pH 7.5. Charges for pS residues at pH 5 were obtained via the electronic structure program Gaussian,[24] with calculations performed at the Hartree−Fock (HF) level of theory with the 6-31G(d)//6-31G(d) basis set. Atomic point charges were assigned with Antechamber[25] and the RESP method.[26] The final atomic point charges used for all pS residues are tabulated in the SI (Tables S1 and S2). For all pS residues, Lennard-Jones (LJ) and bond parameters were obtained from the CHARMM36 force field while angle parameters were obtained from Steinbrecher et al.[23] The SPC/E[27] and INTERFACE[28] force fields were used to model water and the silica surfaces, respectively. The silica surface at pH 7.5 was obtained from the repository provided by Emami et al.[29] and represents a crystalline (100) quartz surface (or silica nanostructures >200 nm). This surface was modified by substituting SiO-Na terminations with SiO-H terminations to construct the surface at pH 5. Further details about the structures of the silica surfaces are contained in the SI. The middle ∼2.5 Å of each silica surface was frozen to prevent extensive deformation during the simulations and to provide a stationary reference for biasing the peptide−surface separation distance as in our prior work.[30]

Six systems (2 pH values × 3 peptide sequences) were assembled with 11 nm of water and one R5 peptide placed in a random initial conformation above an approximately 6.9 × 6.9 × 1.9 nm^3 silica surface, resulting in ∼58,000 atoms in each case (Figures S1 and S2). The surface at pH 7.5 was constructed assuming a solution ionic strength of 0.1−0.3 M, which mimics conditions at physiological pH.[29] Additional Na^+ or Cl^- ions (maximum 8 ions) were added to each system to achieve overall charge neutrality. However, given the number of water molecules in the system (∼16,900), the ions should have a negligible effect on the ionization state of the surface. The additional Na^+ ions (in global pS R5 at pH 5 and 7.5) were modeled with CHARMM36 LJ parameters, unlike surface Na^+ ions that were modeled with INTERFACE LJ parameters. More details about these setups are tabulated in the SI (Table S3) together with an analysis of the interactions between R5 and the two different "types" of Na^+ ions our simulations, the results of which imply that the presence of both types of ions in our simulations likely had negligible effects on our results. Apart from the above-mentioned simulations, we performed two additional simulations at pH 5 with local and global pS R5 exploring the effect of the side chain charge state in phosphoserine (e.g., −1 vs −2), given that phosphoserine has an estimated pK_a of 5.6.[31]

All simulations were conducted using the GROMACS 5.1.2[32] MD simulation engine and PLUMED[33] plugin. A steepest descent energy minimization was performed on all systems. Thereafter, all simulations utilized a 2 fs time step by constraining the bonds between hydrogen and other heavy atoms with the LINCS[34] algorithm. Electrostatic interactions were calculated with the particle mesh Ewald (PME[35]) summation method and a cutoff value of 1.0 nm. A van der Waals cutoff value of 1.0 nm was used along with the Donadio-Bussi-Parrinello thermostat[17] in all simulations.

The enhanced sampling method PTMetaD-WTE[30,36] was used to fully characterize the configurational ensemble of the surface-bound peptides, which is essential in properly simulating these types of complex interfacial systems.[37] First, 24 replicas spanning temperatures of 300 to 450 K[38] were equilibrated in 100 ps parallel tempering (PT) simulations in the NVT ensemble. Then, the systems were sampled in the well-tempered ensemble (WTE) by biasing the potential energy of each system. The σ value (Gaussian hill width) for each system was calculated by dividing in half the equilibrium fluctuations of the potential energy at 300 K (σ values ranged between 310 and 490 kJ/mol, depending on the pH and degree of phosphorylation). Other metadynamics (MetaD) parameters—the bias factor (γ = 10), bias deposition pace (τ = 1 hill/ps), and initial hill height (w_0 = 2.0 kJ/mol)—were constant across all simulations. WTE simulations were deemed converged within 10 ns, resulting in a constant exchange success probability of 34−38% between replicas. Following convergence of the WTE simulations, production MetaD simulations were performed biasing the following collective variables (CVs): (1) the radius of gyration of the peptides' Cα atoms, and (2) the orthogonal distance between the surface and the peptides' centers-of-mass (COMs, calculated using all atoms). The bias factor, hill deposition pace, and initial hill height mentioned above were used. A σ value of 0.1 nm was used for both CVs in all production simulations. As in our previous work,[39] the potential energy was biased with a reduced pace (τ = 1 hill/5 ps) in the production runs. Additionally, a half harmonic restraint (i.e., a "wall") was placed on the distance CV that began

DOI: 10.1021/acs.langmuir.7b02868
Langmuir 2018, 34, 1199−1207

acting on the peptides at a surface separation distance of ∼7.2 nm to limit sampling to one of the two surfaces.

Production simulations were run until convergence was reached, which was considered as the point at which (1) the free energy difference between the adsorbed and solvated states showed $<k_BT$ (∼2.5 kJ/mol) change with simulation time (Figure S3), and (2) the profile of the free energy projected onto the peptide−surface separation distance also showed negligible change with simulation time (data not shown). The systems were considered converged within 250 ns/replica (6 μs total sampling) for simulations of unphosphorylated R5, and within 125 ns/replica (3 μs total sampling) for simulations of phosphorylated R5 peptides. Nonetheless, all simulations were carried out to either 125 or 250 ns/replica depending on the degree of peptide phosphorylation, for consistency. We do note that it is possible that the free energy surfaces could change after additional simulation time (on the order of μs); however, for the time scales simulated herein, these criteria were found to be sufficient for convergence. Additionally, a block averaging analysis was used to calculate the error in the free energy as a function of the CVs biased in the simulations. The results, displayed in Figure S4, show that in each case the error was within 1−2 kJ/mol, which is lower than the level of thermal fluctuations ($=k_BT$) in the systems.

The trajectories from the production runs were visualized using VMD, and the structures of R5 and its variants were clustered using a GROMACS tool. For clustering, the gromos[40] method was used with an RMSD cutoff of 0.10 nm between the radii of gyration of the peptide at each time step. An RMSD cutoff of 0.10 nm was chosen since the radius of gyration free energy profile (see SI) showed several minima 0.15−0.20 nm apart and a small cutoff was needed to differentiate between those structures. In the gromos clustering method, the data point with the largest number of neighbors (defined by a cutoff) is considered the first cluster medoid. Then, this data point and its neighbors are removed from the pool and the algorithm is repeated until all structures have been assigned to a cluster.[41] Thus, each frame is assigned a cluster number.

The unbiased cluster probabilities (denoted by the cluster number above) were obtained using the reweighting method described by Prakash et al.[42] The weight of each frame was given by

$$e^{\beta(V(s,t)-c(t))} \quad (1)$$

where $V(s,t)$ is the instantaneous value of the history-dependent bias potential for the system (s is the value of the CV at a given time t), and $\beta = 1/k_BT$, where k_B is the Boltzmann constant and T is temperature. The reweighting factor, $c(t)$, is a time-dependent offset bias that was calculated on-the-fly using PLUMED. Structures that fell within the particular region of 2D phase space of interest were reweighted and the unbiased probability of the occurrence of a structure in that region of phase space was obtained. We note that the highest-probability structures that are obtained and the probabilities associated with these structures are dependent on the clustering method (e.g., gromos clustering, 0.1 nm cutoff), the number of structures visited by the trajectory, and the convergence of the simulation.

3. RESULTS

3.1. Effect of Phosphorylation on R5/Silica Binding Thermodynamics and Interfacial Peptide Structure.

During our PTMetaD-WTE simulations, different configurations of R5 and its variants were explored with respect to their distance from the surface and radius of gyration. Figure 1 shows the free energy profile along the distance from the surface at pH 7.5. The binding free energy of the peptide to the surface was obtained by subtracting the (thermal) average energy of the bulk region (∼4−5 nm) from the (thermal) average energy of the minima (∼0−1 nm). The binding free energy decreases from approximately −80 kJ/mol for R5 with no pS residues, to −55 kJ/mol for local pS R5, to −30 kJ/mol for global pS R5. Since the decrease in binding free energy is constant (= −25 kJ/mol) when the number of pS residues is increased from 0 to 1 and from 1 to 7, the change in binding free energy is clearly not proportional to the number of pS residues in the sequence of R5. Adding a single pS residue has a dramatic effect on the adsorption thermodynamics, a −25 kJ/mol decrease, as previously mentioned. However, adding additional pS residues does not cause an additional −25 kJ/mol decrease per pS residue, suggesting that the effect (on silica binding strength) of a pS modification is due not only to chemical effects in the side chain, but also sequence effects (i.e., the neighboring residues matter).

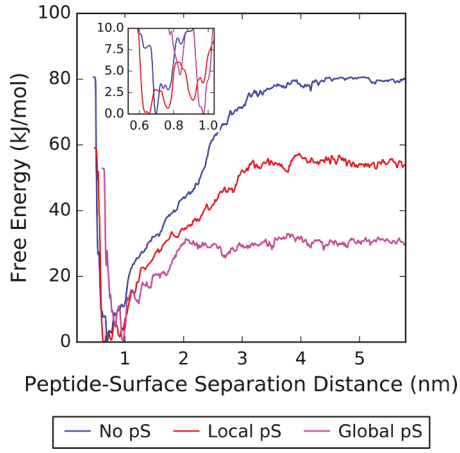

Figure 1. Free energy projected onto the distance between the silica surface at pH 7.5 and the center-of-mass of (blue) R5 without phosphorylation ("No pS"), (red) locally phosphorylated R5 ("Local pS"), and (purple) globally phosphorylated R5 ("Global pS"). A zoomed-in view of the energy minima is shown in the inset.

Apart from altering the binding free energy, the presence of pS residues also changes the preferred structure of R5 at the surface. Figure 1 (inset) highlights preferred locations of the peptides near the surface. The results show that R5, without phosphorylation, prefers being close to the surface at ∼0.68 nm. With a single pS residue, R5 is still able to remain near the surface (energy minima at ∼0.63 and 0.77 nm from the surface). However, a new minimum appears at ∼0.92 nm from the surface. In contrast, global pS R5 singularly prefers to sit away from the surface at ∼0.98 nm. Thus, upon increasing the degree of phosphorylation, R5 prefers to be farther from the surface, resulting in decreased interactions with the surface and consequently decreases in binding free energy. On the other hand, the preferred radius of gyration of R5 decreases with increasing degree of phosphorylation (Figure 2). Figure 2 shows the free energy of R5 along the two biased variables—the radius of gyration and distance from the surface.

To understand the preferred surface separation distances and radii of gyration of R5 and its variants, the trajectories were clustered and reweighted (see Methods section). Reweighting was done in specific regions of interest in CV phase space (i.e., energetic minima on the surface). The top-weighted structures from each clustering analysis in the respective regions of phase space are presented here (Figure 2, bottom). For R5 without pS, the peptide lies close to the surface in extended structures (∼1.2 and 1.6 nm radius of gyration). Electrostatic interactions between positively charged side chains (lysine and arginine residues) and negatively charged adsorption sites on the silica surface allow the peptide to form and retain these extended structures on the surface. The RRIL motif at the C-terminus of R5 (green ribbon, Figure 2) also binds strongly to silica. This

DOI: 10.1021/acs.langmuir.7b02868
Langmuir 2018, 34, 1199−1207

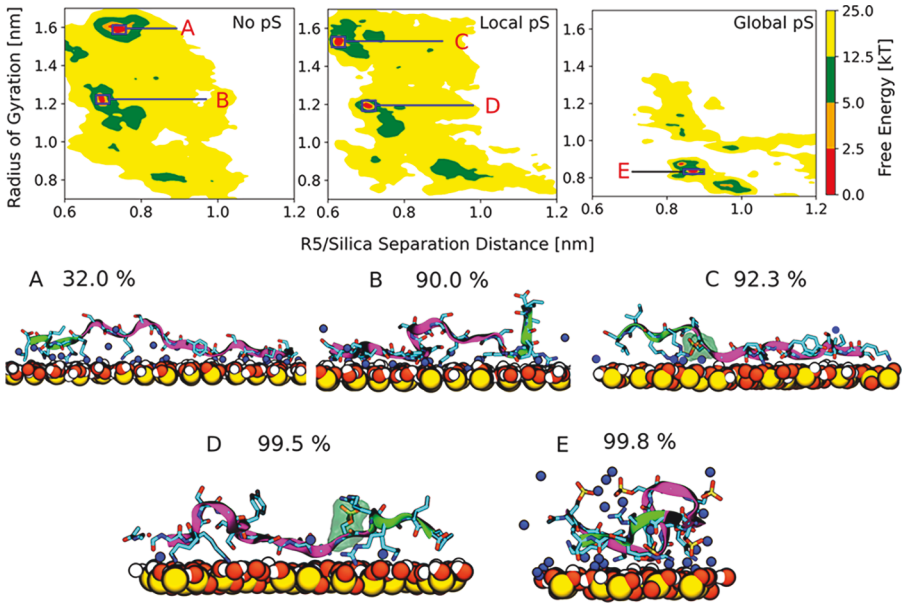

Figure 2. (Top) 2D plot of the free energy projected onto the radius of gyration (Cα atoms) and the distance between the silica surface at pH 7.5 and the center-of-mass of R5 without phosphorylation (left: "No pS"), locally phosphorylated (middle: "Local pS"), and globally phosphorylated (right: "Global pS"). The x-axis is cut off to highlight the surface-bound states only. (Bottom) Conformations of the peptides with the highest probabilities from a clustering analysis of the simulations at pH 7.5 in the regions of the minima shown in the top row, along with the corresponding cluster weights from reweighting. The backbone of the peptides is shown in purple. Cyan, red, yellow, blue, gold, and white coloring correspond to carbon, oxygen, silicon, nitrogen, phosphorus, and surface hydrogen atoms, respectively (peptide hydrogen atoms are not pictured for clarity). Sodium ions are shown in blue, and water is not pictured for clarity. The RRIL motif of the peptides is shown as a green ribbon, and to help identify the lone pS residue in local pS R5, pS is surrounded by a transparent green shell.

motif was shown to be crucial to silica precipitation using unphosphorylated R5 in experiments.[43] The RRIL motif is, however, absent in native silaffin and thus, it can be expected that it will have a negligible role in binding to the surface in our systems with phosphorylated R5 peptides.

Indeed, when a single pS residue is introduced (Figure 2C, D, E), the RRIL motif interacts less strongly/frequently with the surface. This is demonstrated in Figure S5, which shows the free energy profile as a function of the distance between the center-of-mass of the RRIL motif in each peptide and the silica surface (see Figure S6 for pH 5 results). Instead, the RRIL motif in local pS R5 is observed to interact with the lone pS residue in the sequence; either two arginine residues, or one arginine residue and an Na^+ ion, bind to the pS residue to compensate for its −2 charge at pH 7.5. However, the N-terminal residues are free to interact with the surface through their positively charged side chains so that they extend and approach the surface closely (Figure 2C, D).

Global pS R5 prefers a more compact structure (Figure 2E), promoted by increased interactions of intramolecular, charged species (lysine/arginine residues with pS residues), and shows a significant reduction in binding of the RRIL motif to silica (Figures S5, S6). In the case of global pS R5, the pS residues outnumber the positively charged amino acids in the sequence, resulting in an overall negative charge of the peptide. Consequently, some pS residues interact with 2 Na^+ ions in their vicinity to compensate for their −2 charge. Notably, the peptide remains tethered to the surface through pS residues that bind to surface-adsorbed Na^+ ions, albeit with a lesser binding free energy. It is important to note that the adsorption mechanism of global pS R5 to silica is different from unphosphorylated or local pS R5, since the peptide has an overall negative charge and would ordinarily be repelled from the like-charged silica surface. However, the strongly adsorbed surface ions allow the peptide to adsorb close to the surface.

3.2. Effect of pH on the Mechanism of R5/Silica Binding. Since biosilicification is a pH-sensitive process, it is crucial to investigate the effects of pH on R5/silica binding. Figure 3 shows the free energy profile for the adsorption of R5 and its variants to the silica surface at pH 5. The free energy profiles at pH 7.5 are also plotted to facilitate comparison. Markedly, all peptide sequences bind with lesser binding free

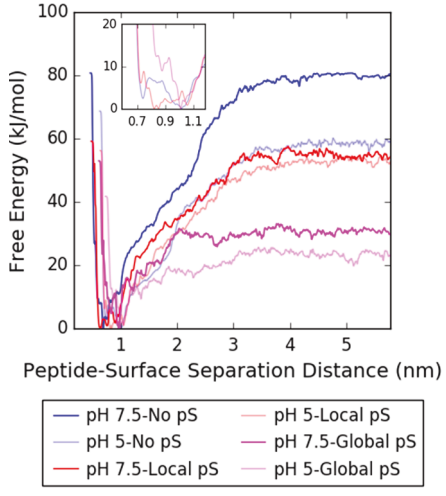

Figure 3. Free energy projected onto the distance between the silica surface at (dark colors) pH 7.5 and (light colors) pH 5 and the center-of-mass of (blue) R5 without phosphorylation ("No pS"), (red) locally phosphorylated R5 ("Local pS"), and (purple) globally phosphorylated R5 ("Global pS"). A zoomed-in view of the energy minima for the pH 5 simulations only is shown in the inset.

DOI: 10.1021/acs.langmuir.7b02868
Langmuir 2018, 34, 1199−1207

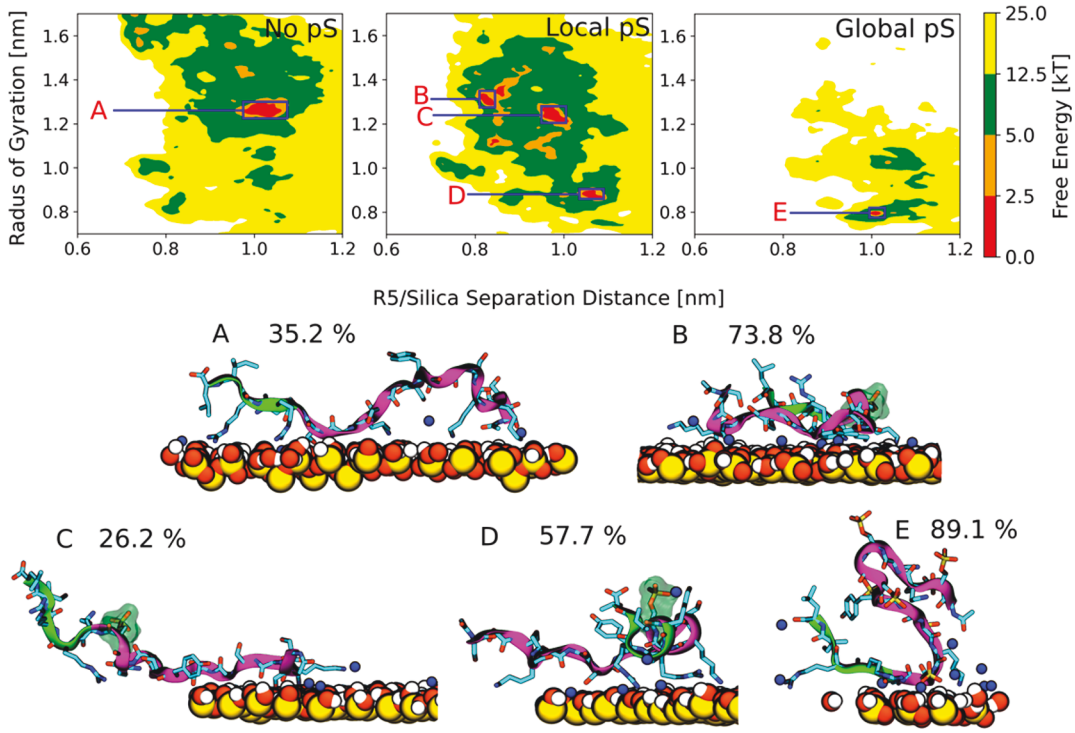

Figure 4. (Top) 2D plots of the free energy projected onto the distance between the silica surface at pH 5 and the center-of-mass of R5 without phosphorylation (left: "No pS"), locally phosphorylated (middle: "Local pS"), and globally phosphorylated (right: "Global pS"), as a function of the radius of gyration of the Cα atoms in R5. The *x*-axis is cut off to highlight the surface-bound states only. (Bottom) Conformations of the peptides with the highest probabilities from the clustering analysis of the simulations at pH 5 in the regions of the above-shown minima, along with the corresponding cluster weights from reweighting. Minima correspond to low free energy states indicated in the plots in the top row. Coloring is the same as described in Figure 2.

energy at pH 5 than at pH 7.5. The decrease in binding free energy is greatest for R5 without phosphorylation. The magnitude of the decrease in binding free energy (= 23 kJ/mol) is comparable to the decrease upon introducing one pS residue into the peptide sequence (= 25 kJ/mol). Conversely, both local and global pS R5 show a much smaller decrease in the binding free energy (= 0−10 kJ/mol).

Looking closely at the free energy minima (Figure 3, inset), we find that as the degree of phosphorylation increases, the peptides preferentially adsorb at distances farther away from the surface. The same trend was evident from observing the free energy minima at pH 7.5 (Figure 1, inset). Like the case at pH 7.5, these increases in the surface separation distances of the peptides correlate with decreases in their binding free energies to silica at pH 5 (Figure 3). When R5 is unphosphorylated at pH 5, the peptide favorably resides in two minima at distances of ∼0.73 and 1.0 nm (n.b., a single minimum was observed at ∼0.68 nm at pH 7.5). This shift toward larger peptide−surface separation distances is likely the cause for the sizable decrease in binding free energy observed upon adsorption of unphosphorylated R5 to silica at pH 5 versus at pH 7.5. Local pS R5 exhibits three minima at pH 5 at distances of ∼0.80, 0.85, and 1.05 nm, which is a less dramatic departure from its behavior at pH 7.5 (n.b., three minima at ∼0.63, 0.77, and 0.92 nm from the surface) compared to unphosphorylated R5, explaining the smaller decrease in binding free energy in moving from pH 7.5 to pH 5. Finally, global pS R5 prefers to remain farther from the surface at a distance of ∼1.0 nm (like its behavior at pH 7.5 with a single minimum at ∼0.98 nm from the surface).

From the 2D free energy profiles along the distance from the surface and radius of gyration (Figure 4), it is evident that the preferred radius of gyration decreases as the degree of phosphorylation increases, mimicking the behavior of R5 at pH 7.5. However, some differences do exist. For the case of the unphosphorylated peptide, the minimum at a radius of gyration of ∼1.6 nm at pH 7.5 (Figure 2) is largely absent at pH 5 (Figure 4). Instead, the minimum at 1.2 nm is much larger. For local pS R5, the number of minima increases from pH 7.5 to pH 5, and the preference shifts toward a lower radius of gyration and greater distance from the surface. Moreover, the free energy surface at pH 5 is more diffuse and exhibits numerous small minima.

These findings necessitate an investigation of the structure of R5 and its variants, like the analysis for pH 7.5 (Figure 4, bottom). At pH 5, due to changes in the ionization state of the surface, fewer negatively charged surface sites are available for adsorption of positively charged side chains in R5. With fewer interaction sites, R5 binds weakly to the surface—a trend that is evident in the overall decrease in binding free energy of all the peptides. These differences in the ionization state of the surfaces are directly reflected in the surface-bound configurations of R5 in Figure 4. Although all positively charged side chains bind to the surface at both pHs, other residues do not interact with the surface at pH 5, which prevents full extension of the peptide on the surface. At pH 5, the central residues hydrogen-bond with nearby water molecules instead of interacting with surface-bound Na^+ ions. The lack of Na^+ ions on the surface is directly correlated with the lack of surface adsorption sites and the surface ionization state. Additionally, as seen at pH 7.5 (Figure 2), the introduction

DOI: 10.1021/acs.langmuir.7b02868
Langmuir 2018, 34, 1199−1207

of pS residues forces the peptide into more compact structures due to intramolecular interactions of pS and lysine/arginine residues (Figure 4). In fact, R5 can even adopt a partially helical structure (Figure 4D.)

3.3. Effect of the pS Side Chain Protonation State on R5/Silica Binding. To understand how the observed differences in the binding free energies of the peptides at pH 5 and pH 7.5 are arising—i.e., to determine whether they are solely due to differences in the ionization state of the surfaces or pK_a differences of the pS side chain (−2 charge at pH 7.5 vs −1 charge at pH 5)—two additional PTMetaD-WTE simulations were performed of local and global pS R5 at pH 5 with pS residues constructed to have a −2 overall charge. These simulations were carried out in the same manner, with the same parameters, and for the same length of time as previous simulations for consistency (see Methods section). Figure 5 shows a comparison of the change in free energy upon adsorption of local and global pS R5, with both side chain protonation states, to the silica surface at pH 5.

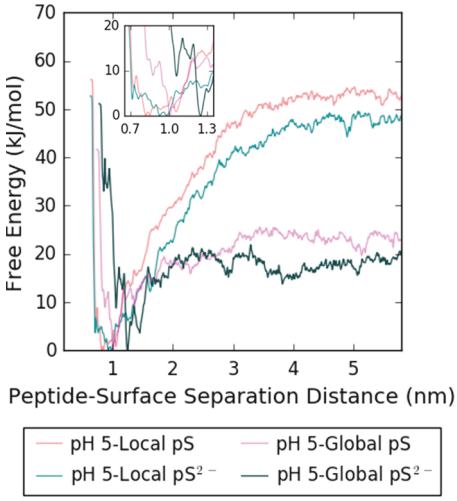

Figure 5. Free energy projected onto the distance between the silica surface at pH 5 and the center-of-mass of local pS R5 with a pS charge state of −1 (red) and −2 (light green), and global pS R5 with a pS charge state of −1 (purple) and −2 (dark green). A zoomed-in view of the energy minima is shown in the inset.

The results (Figure 5) show that the change in pS protonation state affects the binding free energy of local and global pS R5 to silica by ∼3−5 kJ/mol, or by approximately 10% in either case. These findings suggest that in addition to the surface chemistry effect, observed differences in the adsorption thermodynamics at pH 5 versus at pH 7.5 are also affected by the protonation state of the pS side chain. Changing the protonation state of the pS side chain so that it has a charge of −2 (state at pH 7.5) instead of −1 (state at pH 5), still provides a diffuse 2D free energy surface (like Figure 4, local pS). As shown in Figure 6, R5 shows only one accessible minimum which is close to the surface where it adopts an extended structure. However, the free energy surface has several other regions which might be accessible, within our free energy error. Unlike its behavior at the −1 protonation state, the free energy surface does not have multiple low energy minima.

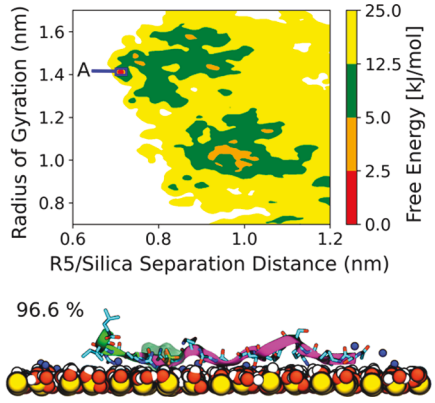

Figure 6. (Top row) 2D plot of the free energy projected onto the distance between the silica surface at pH 5 for local pS R5 (pS charge of −2). The *x*-axis is cut off to highlight the surface-bound states only. (Bottom rows) Top weighted surface-bound peptide conformations from a clustering analysis of the structures in the free energy minimum labeled as A in the plot above. Coloring is the same as described in Figure 2.

4. DISCUSSION

In peptide-mediated silica formation, cationic peptides like R5 are thought to aid the process at different stages. In the early stages of silica formation, these peptides promote condensation of silicic acid into polysilicic acid.[5] It is suggested that the peptides form templates where condensation can take place, but that sometimes the peptides themselves get encapsulated by silica.[3,43,44] Therefore, an alternative pathway for peptide-mediated biomineral formation may exist where precursors of the biomineral itself—or some other interface that is present (i.e., the air/water interface[16])—bind silaffin-based peptides and facilitate peptide templating, which in turn leads to biomineral nanostructure formation.[45] Finally, cationic peptides are thought to induce flocculation of silica particles, by reducing the energy barrier for the growth of nuclei and thus promoting the growth of silica nanostructures.[5] To attain the desired yield and morphology of silica nanostructures from *in vitro* silicification, it is important to understand the forces that dominate every stage of this process. The interaction of peptides with silica is crucial to all stages of biosilicification.

In this paper, we investigated the interaction of silica with R5—a commonly used peptide for *in vitro* silicification—with varying degrees of phosphorylation. It has been shown that unphosphorylated R5 precipitates silica at neutral pH, but loses this ability at acidic pHs. Therefore, we analyzed the binding thermodynamics and structure of R5 at both pH 7.5 and pH 5. Our results show that unphosphorylated R5 binds much more strongly to silica at pH 7.5 than pH 5, by approximately −23 kJ/mol. In fact, at pH 7.5, the peptide adopts extended structures on the surface, maximizing interactions of its positively charged side chains (i.e., lysine and arginine residues) with the surface. This also enables it to adopt a position close to the surface. On the other hand, unphosphorylated R5 assumes a more compact structure on the surface at pH 5. At acidic pH, it is unable to find the same number of charged surface sites for adsorption as at pH 7.5, forcing the central residues to instead interact with nearby water molecules. The C-terminus RRIL motif that is implicated in the precipitation of silica nanostructures does not interact with the surface completely at pH 5. Therefore, we suggest that the inability of unphosphorylated R5 to assemble silica at pH 5 results from

DOI: 10.1021/acs.langmuir.7b02868
Langmuir 2018, 34, 1199−1207

the changing ionization state of the surface that reduces the tendency of the peptide to interact with the silica surface. We note that the binding free energy of unphosphorylated R5 to silica at pH 5 is approximately the same as that of local pS R5 at pH 7.5, which was able to precipitate silica in experiments. Therefore, we further suggest that the inability of R5 to fully extend on the surface at pH 5 hinders or impairs the formation of peptide templates on the surface.

Another area of interest in R5/silaffin biosilicification has been to understand the effect of post-translational modifications (PTMs) of the peptide sequence, such as phosphorylation or hydroxylation, on the silica precipitating activity of the peptides. Recently, Lechner et al.[11] phosphorylated the serine residues of R5 and measured the silica precipitating activity of a number of variants of R5 at neutral pH. R5, without modifications, precipitated silica nanospheres. However, on phosphorylating one and seven serine residues in R5, silica yields were drastically reduced to 38.8% and 0.6%, respectively, with singly phosphorylated R5 yielding poorly formed silica nanostructures. Our results highlight the effect of phosphorylation on the molecular scale, hoping to shed light on the differences observed by Lechner et al. We find a clear trend of decreasing binding free energy to silica for an increasing degree of phosphorylation of the R5 peptide sequence. This trend remains the same at both neutral and acidic pHs. Global pS binds the least strongly of all three variants and is expected to yield the lowest amount of silica—confirmed by the results of Lechner et al. This is intuitive given the negative charges of both global pS R5 and the silica surface. However, in contrast to the hypothesis by Lechner et al. of a purely repulsive interaction between global pS R5 and silica, we see a minimum binding free energy of −30 kJ/mol, predominantly due to interactions between global pS R5 and surface-bound ions. While the experimental and computational trends match in this case, it is not straightforward to assume that tight-binders to silica always precipitate the most silica. To this point, Patwardhan et al.[46] suggest that cationic peptides that bind strongly to silica perform poorly in early stages of silica precipitation. Limo and Perry[47] also argue that peptide−surface binding may not be the primary indicator of the biomineralization efficiency of a given peptide.

Nonetheless, details about the atomic-level interactions in these simulations can provide information useful to interpret these experiments. With a single pS residue introduced into the peptide sequence, the peptide remains cationic and we observe a binding free energy of −55 kJ/mol to silica at pH 7.5. Our results show that the binding free energy of local pS R5 is reduced compared to unphosphorylated R5 due to intramolecular interactions between nearby arginine and pS residues in the sequence of local pS R5. From our analysis of the surface-bound structures of R5, it is evident that it is primarily the binding of the C-terminus RRIL motif that is different between the unphosphorylated and locally phosphorylated peptides, suggesting a cause for the disruption in nanostructure formation and reduced silica yield observed with local pS R5 in the experiments by Lechner et al. Thus, our findings provide support for the previously proposed observation that the RRIL motif of R5 is important for *in vitro* silica precipitation.

5. CONCLUSIONS

Our study has highlighted some of the dominant driving forces that may contribute to the precipitation of silica and the formation of nanostructures in the biosilicification process. We find that the binding free energy of R5 to the silica surface decreases with decreasing pH and an increasing degree of phosphorylation. These differences are due to alterations in the electrostatic interactions between the peptide and the surface or electrolyte ions, and to intramolecular hydrogen-bonding that dictates the binding between R5 (and its variants) with the silica surface at different pH conditions. At acidic pHs, the terminal chemistry of the surface dominates by forcing the peptide to interact with itself (independent of the degree of phosphorylation). However, at neutral pH, the degree of phosphorylation dominates the nature of R5 binding to silica, dictating the level of both self- and surface-interactions.

Our predictions of the nature of the interactions of R5 with silica highlights important molecular-scale features, such as the role of the C-terminal RRIL motif, the surface-repulsion of R5 at acidic pHs, the interaction of pS residues with the peptide/silica environment, and the facilitation of peptide−surface binding through surface-bound Na^+ ions. These results are crucial not only to understand previous experiments of the same nature (i.e., Lechner et al.) but also to predict how modifications of specific residues might affect the silica precipitating activity of the peptide. We hope our findings can serve as a guide for future experimental and theoretical efforts to direct bioinspired silicification toward the design of new biomaterials and biotechnologies.

■ ASSOCIATED CONTENT

Supporting Information

The Supporting Information is available free of charge on the ACS Publications website at DOI: 10.1021/acs.langmuir.7b02868.

Phosphoserine parameterization; silica surface description; initial coordinates; simulated systems parameters; ion-peptide interaction analysis; convergence assessment and error analysis; RRIL binding (PDF)

■ AUTHOR INFORMATION

Corresponding Author

*E-mail: jpfaendt@uw.edu.

ORCID

Gary Drobny: 0000-0002-7293-1897

Jim Pfaendtner: 0000-0001-6727-2957

Author Contributions

#K. G. Sprenger and Arushi Prakash contributed equally to this work.

Notes

The authors declare no competing financial interest.

■ ACKNOWLEDGMENTS

J.P. and K.G.S. acknowledge the support of NSF award CBET-1264459. J.P. and G.D. acknowledge support of NSF award MCB-1715123. This work was facilitated using computational, storage, and networking infrastructure provided by the Hyak supercomputer system, supported in part by the University of Washington and the UW Student Technology Fee Proposal program (award 2015-028) and NSF MRI program CHE-1624430.

DOI: 10.1021/acs.langmuir.7b02868
Langmuir 2018, 34, 1199−1207

REFERENCES

(1) Lechner, C. C.; Becker, C. F. W. Modified silaffin R5 peptides enable encapsulation and release of cargo molecules from biomimetic silica particles. *Bioorg. Med. Chem.* **2013**, *21* (12), 3533−3541.

(2) Otzen, D. The role of proteins in biosilicification. *Scientifica* **2012**, *2012*, 1.

(3) Knecht, M. R.; Wright, D. W. Functional analysis of the biomimetic silica precipitating activity of the R5 peptide from Cylindrotheca fusiformis. *Chem. Commun.* **2003**, *24*, 3038−3039.

(4) Ndao, M.; Goobes, G.; Emani, P. S.; Drobny, G. P. A REDOR ssNMR Investigation of the Role of an N-Terminus Lysine in R5 Silica Recognition. *Langmuir* **2016**, DOI: 10.1021/acs.langmuir.5b04114.

(5) Senior, L.; Crump, M. P.; Christopher, W.; Booth, P. J.; Mann, S.; Perriman, A. W.; Curnow, P.; Chen, C. L.; Rosi, N. L.; Sarikaya, M.; Temerler, C.; Jen, A. K. Y.; Schulten, K.; Baneyx, F.; Mann, S.; Naik, R. R.; Whitlock, P. W.; Rodriguez, F.; Brott, L. L.; Glawe, D. D. Structure and function of the silicifying peptide R5. *J. Mater. Chem. B* **2015**, *3* (13), 2607−2614.

(6) Roehrich, A.; Ash, J.; Zane, A.; Masica, D. L.; Gray, J. J.; Goobes, G.; Drobny, G. Solid-State NMR Studies of Biomineralization Peptides and Proteins. In *Proteins at Interfaces III State of the Art*; American Chemical Society, 2012; Vol. *1120*, pp 77−96.

(7) Kröger, N.; Lorenz, S.; Brunner, E.; Sumper, M. Self-assembly of highly phosphorylated silaffins and their function in biosilica morphogenesis. *Science* **2002**, *298* (5593), 584−586.

(8) Kröger, N.; Deutzmann, R.; Bergsdorf, C.; Sumper, M. Species-specific polyamines from diatoms control silica morphology. *Proc. Natl. Acad. Sci. U. S. A.* **2000**, *97* (26), 14133−14138.

(9) Sumper, M.; Kröger, N. Silica formation in diatoms: the function of long-chain polyamines and silaffins. *J. Mater. Chem.* **2004**, *14* (14), 2059−2065.

(10) Poulsen, N.; Kröger, N. Silica morphogenesis by alternative processing of silaffins in the diatom Thalassiosira pseudonana. *J. Biol. Chem.* **2004**, *279* (41), 42993−42999.

(11) Lechner, C. C.; Becker, C. F. W. Exploring the effect of native and artificial peptide modifications on silaffin induced silica precipitation. *Chemical Science* **2012**, *3* (12), 3500−3504.

(12) Rodríguez, F.; Glawe, D. D.; Naik, R. R.; Hallinan, K. P.; Stone, M. O. Study of the chemical and physical influences upon in vitro peptide-mediated silica formation. *Biomacromolecules* **2004**, *5* (2), 261−265.

(13) Lenoci, L.; Camp, P. J. Self-assembly of peptide scaffolds in biosilica formation: computer simulations of a coarse-grained model. *J. Am. Chem. Soc.* **2006**, *128* (31), 10111−10117.

(14) Kröger, N.; Deutzmann, R.; Sumper, M. Polycationic peptides from diatom biosilica that direct silica nanosphere formation. *Science* **1999**, *286* (5442), 1129−1132.

(15) Eby, D. M.; Johnson, G. R.; Farmer, B. L.; Pandey, R. B. Supramolecular assembly of a biomineralizing antimicrobial peptide in coarse-grained Monte Carlo simulations. *Phys. Chem. Chem. Phys.* **2011**, *13* (3), 1123−1130.

(16) Lutz, H.; Jaeger, V.; Schmüser, L.; Bonn, M.; Pfaendtner, J.; Weidner, T. The Structure of the Diatom Silaffin Peptide R5 within Freestanding Two-Dimensional Biosilica Sheets. *Angew. Chem., Int. Ed.* **2017**, *56* (28), 8277−8280.

(17) Bussi, G.; Davide, D.; Michele, P. Canonical sampling through velocity rescaling. *J. Chem. Phys.* **2007**, *126* (1), 014101.

(18) Schwierz, N.; Horinek, D.; Liese, S.; Pirzer, T.; Balzer, B. N.; Hugel, T.; Netz, R. R. On the relationship between peptide adsorption resistance and surface contact angle: a combined experimental and simulation single-molecule study. *J. Am. Chem. Soc.* **2012**, *134* (48), 19628−19638.

(19) Sultan, A. M.; Westcott, Z. C.; Hughes, Z. E.; Palafox-Hernandez, J. P.; Giesa, T.; Puddu, V.; Buehler, M. J.; Perry, C. C.; Walsh, T. R. Aqueous Peptide−TiO2 Interfaces: Isoenergetic Binding via Either Entropically or Enthalpically Driven Mechanisms. *ACS Appl. Mater. Interfaces* **2016**, *8* (28), 18620−18630.

(20) Wright, L. B.; Palafox-Hernandez, J. P.; Rodger, P. M.; Corni, S.; Walsh, T. R. Facet selectivity in gold binding peptides: exploiting interfacial water structure. *Chemical Science* **2015**, *6* (9), 5204−5214.

(21) Humphrey, W.; Dalke, A.; Schulten, K. VMD: Visual molecular dynamics. *J. Mol. Graphics* **1996**, *14* (1), 33−38.

(22) Huang, J.; MacKerell, A. D. CHARMM36 all-atom additive protein force field: Validation based on comparison to NMR data. *J. Comput. Chem.* **2013**, *34* (25), 2135−2145.

(23) Steinbrecher, T.; Latzer, J.; Case, D. A. Revised AMBER parameters for bioorganic phosphates. *J. Chem. Theory Comput.* **2012**, *8* (11), 4405−4412.

(24) Frisch, M. J.; Trucks, G. W.; Schlegel, H. B.; Scuseria, G. E.; Robb, M. A.; Cheeseman, J. R.; Scalmani, G.; Barone, V.; Mennucci, B.; Petersson, G. A.; et al., *Gaussian 09*, Revision B.01; Wallingford, CT, 2009.

(25) Wang, J. W.; Kollman, P. A.; Case, D. A. Automatic atom type and bond type perception in molecular mechanical calculations. *J. Mol. Graphics Modell.* **2006**, *25*, 247−260.

(26) Cornell, W. D.; Cieplak, P.; Bayly, C. I.; Kollmann, P. A. Application of RESP charges to calculate conformational energies, hydrogen-bond energies, and free-energies of solvation. *J. Am. Chem. Soc.* **1993**, *115* (21), 9620−9631.

(27) Berendsen, H. J. C.; Postma, J. P. M.; van Gunsteren, W. F.; Hermans, J., Interaction Models for Water in Relation to Protein Hydration. In *Intermolecular Forces: Proceedings of the Fourteenth Jerusalem Symposium on Quantum Chemistry and Biochemistry Held in Jerusalem, Israel, April 13−16, 1981*, Pullman, B., Ed.; Springer Netherlands: Dordrecht, 1981; pp 331−342.

(28) Heinz, H. a. L. T.-J. a. Thermodynamically Consistent Force Fields for the Assembly of Inorganic, Organic, and Biological Nanostructures: The INTERFACE Force Field. *Langmuir* **2013**, *29* (6), 1754−1765.

(29) Emami, F. S.; Puddu, V.; Berry, R. J.; Varshney, V.; Patwardhan, S. V.; Perry, C. C.; Heinz, H. Force field and a surface model database for silica to simulate interfacial properties in atomic resolution. *Chem. Mater.* **2014**, *26* (8), 2647−2658.

(30) Deighan, M.; Pfaendtner, J. Exhaustively Sampling Peptide Adsorption with Metadynamics. *Langmuir* **2013**, *29* (25), 7999−8009.

(31) Xie, Y.; Jiang, Y.; Ben-Amotz, D. Detection of amino acid and peptide phosphate protonation using Raman spectroscopy. *Anal. Biochem.* **2005**, *343* (2), 223−30.

(32) Abraham, M. J.; Murtola, T.; Schulz, R.; Pall, S.; Smith, J. C.; Hess, B.; Lindahl, E. GROMACS: High performance molecular simulations through multi-level parallelism from laptops to supercomputers. *SoftwareX* **2015**, *1*, 19−25.

(33) Tribello, G. A.; Bonomi, M.; Branduardi, D.; Camilloni, C.; Bussi, G. PLUMED 2: New feathers for an old bird. *Comput. Phys. Commun.* **2014**, *185* (2), 604−613.

(34) Hess, B.; Bekker, H.; Berendsen, H. J. C.; Fraaije, J. G. E. M. LINCS: A linear constraint solver for molecular simulations. *J. Comput. Chem.* **1997**, *18* (12), 1463−1472.

(35) Darden, T.; York, D.; Pedersen, L. Particle mesh Ewald: An N·log(N) method for Ewald sums in large systems. *J. Chem. Phys.* **1993**, *98* (12), 10089−10092.

(36) Bonomi, M.; Parrinello, M. Enhanced Sampling in the Well-Tempered Ensemble. *Phys. Rev. Lett.* **2010**, *104* (19), 190601.

(37) Walsh, T. R. Pathways to Structure−Property Relationships of Peptide−Materials Interfaces: Challenges in Predicting Molecular Structures. *Acc. Chem. Res.* **2017**, *50* (7), 1617−1624.

(38) Prakash, M. K.; Barducci, A.; Parrinello, M. Replica Temperatures for Uniform Exchange and Efficient Roundtrip Times in Explicit Solvent Parallel Tempering Simulations. *J. Chem. Theory Comput.* **2011**, *7* (7), 2025−2027.

(39) Sprenger, K. G.; Pfaendtner, J. Strong Electrostatic Interactions Lead to Entropically Favorable Binding of Peptides to Charged Surfaces. *Langmuir* **2016**, *32* (22), 5690−5701.

(40) Daura, X.; Gademann, K.; Jaun, B.; Seebach, D.; van Gunsteren, W. F.; Mark, A. E. Peptide folding: when simulation meets experiment. *Angew. Chem., Int. Ed.* **1999**, *38* (1−2), 236−240.

DOI: 10.1021/acs.langmuir.7b02868
Langmuir 2018, 34, 1199−1207

(41) Fraccalvieri, D.; Pandini, A.; Stella, F.; Bonati, L. Conformational and functional analysis of molecular dynamics trajectories by Self-Organising Maps. *BMC Bioinf.* **2011**, *12* (1), 158.
(42) Prakash, A.; Sprenger, K. G.; Pfaendtner, J. Essential slow degrees of freedom in protein-surface simulations: A metadynamics investigation. *Biochem. Biophys. Res. Commun.*, **2017**. DOI: 10.1016/j.bbrc.2017.07.066
(43) Lechner, C. C.; Becker, C. F. W. A sequence-function analysis of the silica precipitating silaffin R5 peptide. *J. Pept. Sci.* **2014**, *20* (2), 152−158.
(44) Ravera, E.; Cerofolini, L.; Martelli, T.; Louka, A.; Fragai, M.; Luchinat, C. (1)H-detected solid-state NMR of proteins entrapped in bioinspired silica: a new tool for biomaterials characterization. *Sci. Rep.* **2016**, *6*, 27851.
(45) Kharlampieva, E.; Jung, C. M.; Kozlovskaya, V.; Tsukruk, V. V. Secondary structure of silaffin at interfaces and titania formation. *J. Mater. Chem.* **2010**, *20* (25), 5242−5250.
(46) Patwardhan, S. V.; Emami, F. S.; Berry, R. J.; Jones, S. E.; Naik, R. R.; Deschaume, O.; Heinz, H.; Perry, C. C. Chemistry of aqueous silica nanoparticle surfaces and the mechanism of selective peptide adsorption. *J. Am. Chem. Soc.* **2012**, *134* (14), 6244−6256.
(47) Limo, M. J.; Perry, C. C. Thermodynamic study of interactions between ZnO and ZnO binding peptides using isothermal titration calorimetry. *Langmuir* **2015**, *31* (24), 6814−6822.

DOI: 10.1021/acs.langmuir.7b02868
Langmuir 2018, 34, 1199−1207